Journal of Solid Mechanics Vol. 17, No. 1 (2025) pp. 98-114
DOI: 10.60664/jsm.2025.1187204

Research Paper

Torsional Vibration and Sensitivity Analysis of Marine Propeller Shaft Using Hybrid Modeling

S. Soheili [1*], S.E. Hosseini [2]

[1]*Department of Mechanical Engineering, Mashhad Branch, Islamic Azad University, Mashhad, Iran*
[2]*Department of Mechanical Engineering, Imam Hossein University, Tehran, Iran*

Received 18 October 2024; Received in revised form 28 April 2025; Accepted 5 May 2025

ABSTRACT

This paper investigates the modeling of torsional vibration of marine shaft systems using the distributed-lumped (hybrid) modeling technique (DLMT). A new analytical method is employed to solve the equation of motion for the shaft torsional vibrations, and the solution is modeled as a series of interconnected distributed and lumped elements. The DLMT is then utilized to calculate the natural frequencies of a rotor system with various elements, and the results are compared and verified with the results of other techniques, such as the finite element method (FEM), using ANSYS software. A marine propeller shaft with multiple elements such as different couplings and flanges is then modeled and analyzed by the DLMT to obtain the natural frequencies. The results are compared and verified with the frequencies and mode shapes obtained by KissSoft software. In addition, the sensitivity analysis of significant parameters such as coupling stiffness, propeller moment of inertia, and shaft diameter are also implemented. The results show that the presented method can be simply and effectively applied to complicated systems, and brings highly accurate results.

Keywords: Torsional vibration*;* Hybrid modeling*;* Marine propeller shaft*;* Distributed element*;* Lumped element.

1 INTRODUCTION

THE question of vibration modeling of industrial systems, especially rotating shafts, is one of the basic considerations in the engineering design of dynamic systems. Not only the avoidance from natural frequencies of such systems have been noticed since long before, but the condition monitoring (CM) and fault detection of highly sensitive and expensive plants such as marine propulsion and turbine systems are widely employed using accurate vibration models of systems [1]. Condition Monitoring for rotating machinery incorporates a wide range of

*Corresponding author. Tel.: +98 51 36625046, Fax: +98 51 36627560.
E-mail address: soheili@iau.ac.ir (S. Soheili)

techniques. Developments are continually made with the use of new analysis methods, increased computing power, measurement techniques, and so on. Different analytical solutions are proposed for the simple cases of vibrating systems. However, there is no analytical and precise method for vibration modeling of the complicated systems combined of various shaft and disk elements; such as gears, propellers, pulleys, and so on. In such cases, the proposed techniques widely utilize the numerical and approximate methods, such as Taylor series [2]; spring-mass-damper models, such as the ones mentioned in references [3, 4]; or transfer matrix method (TMM) and finite element method (FEM), such as references [5, 6]. There are some other techniques of vibration modeling, such as the shear wave propagation method, which are mostly used for viscoelastic structures comprising fiber-reinforced piezoelectric composite materials [7-9]. Among different methods of modeling systems such as lumped-lumped modeling technique (LLMT) and distributed-lumped modeling technique (DLMT), or numerical and approximate methods such as TMM and FEM, it is clear that the model combined with both the distributed and lumped elements is the best representative of complex and accurate systems.

The distributed-lumped modeling technique (hybrid modeling) was firstly introduced by Whalley [10] for second order systems. This technique was applied by Aleyaasin et al. [11] for calculating the flexural frequencies of Euler-Bernoulli beams using 4×4 matrices. Recently, DLMT was employed to investigate the flexural vibration of a multi-step turbine shaft using Timoshenko beam theory [12]. The distributed-lumped method can also be applied to other systems, such as modeling the torsional [13] and axial [14] vibrations and calculating frequency and time responses in forced systems. Three types of vibrations occur in marine propulsion systems: torsional, longitudinal, and lateral vibrations. Torsional vibrations are usually induced by motor torque changes, propeller torque fluctuations, and the torsional elasticity of transmission systems [15,16]. Torsional vibrations are the most dangerous type for the shaft line, crankshaft and bearings [17]. Huang and Horng [18] used the TMM for torsional vibration analysis of damped systems. Free and forced torsional vibration problems are studied by Wu and Yang [19] for the multidegree of freedom system using the TMM. The FEM is also utilized for torsional vibration analysis of marine propulsion systems [20-22]. Furthermore, some studies on torsional, longitudinal, and transverse vibration were evaluated by experiments [23,24]. Han et al. [25[investigated the effects of some parameters such as the stiffness of the joints and shaft and the damping of the connections and shaft for marine propulsion systems. In addition, the combined torsional, longitudinal and flexural vibrations and their interactions are also investigated by some researchers [26]. Among different methods of vibration modeling, the most important advantage of the DLMT, compared with the FEM, is the reduced size of matrices and equations. The transfer matrix order of the entire system in the DLMT is 2×2, while in FEM, the stiffness matrix is a 2(n+1)×2(n+1) matrix for n elements. Compared with TMM, the DLMT employs the exact solution of the equation of motion to obtain the transfer matrix of the distributed element, therefore, there is no approximation in this method, and the natural frequencies and mode shapes are the exact ones.

In this study, a method based on the distributed lumped modeling approach is proposed to solve the governing equations of motion for the torsional vibration. The method is then employed to model a general three–stage distributed-lumped-distributed system with clamped-free boundary conditions (BCs), which are more common in real systems. To check the correctness and accuracy of the present method, natural frequencies of the system achieved by this method are compared with those obtained by FEM utilizing ANSYS software, and also the numerical Holzer method. The DLMT method is then employed to obtain the frequencies of a marine propulsion system, and the results are compared with KissSoft software outcomes. The mode shapes of the propeller shaft system are also presented, and the sensitivity analysis of significant parameters is implemented.

The main novelty of this paper is the methodology proposed for the modeling of torsional vibrations of continuous shafts with multiple elements, precisely and without approximations. As mentioned before, in contrast with the other methods such as FEM and TMM, the DLMT deals with the shaft as one continuous element with inertia and elastic effects, and since the presented matrix form is based on the main solution of governing equations, no approximation is utilized. Therefore, mathematically or physically; neither simplification nor approximation has been taken into account. It is shown how the whole model of the system is obtained simply by multiplication of a series of interconnected distributed and lumped elements. The method of applying the boundary conditions (BCs) and the technique of obtaining the frequency response of the system are also presented. Another novelty of this paper is the application of DLMT for the exact modeling of marine propeller shaft as a complicated system with multiple elements such as the elastic couplings, the engines and the thrust bearing; and an in-depth study of the various parameters with comparative graphical descriptions.

2 THE GENERAL DISTRIBUTED-LUMPED MODEL

Generally speaking, systems in the hybrid modeling technique are considered as the combination of two types of elements:

1) The distributed element, which is the main part of shafts and rotors; with the distributed mass or inertia.
2) The lumped element, which is the supplementary part of shafts and rotors; with the concentrated mass or inertia such as disks, gears, propellers, pulleys, and so on.

In this way, a system is considered as a combined set of distributed and lumped elements, in which the final vibration model of the system is obtained by setting the distributed and lumped matrices of different parts and combining them together (see Fig. 1). Distributed and lumped matrices are formed according to the analytical equations of motion, so this is the highly accurate technique in contrast with the other approximate techniques such as TMM (based on lumped elements), FEM, and so on. Another advantage of this technique is that the continuity conditions between elements are simply satisfied, and only the boundary conditions (BCs) of the system should be applied to the model.

2.1 The transfer matrix for distributed element

The equations of motion for the torsional vibration of a rod with the density ρ, the shear modulus of elasticity G and the polar moment of inertia J can be expressed by the following equations (e.g., see [27, 28]):

$$\frac{\partial T(x,t)}{\partial x} = \rho J \frac{\partial^2 \theta(x,t)}{\partial t^2} \tag{1}$$

$$\frac{\partial \theta(x,t)}{\partial x} = \frac{1}{GJ} T(x,t) \tag{2}$$

where $\theta(x,t)$ and $T(x,t)$ are the torsional angle and torque functions, respectively; x is the distance along a section and t is time.

Differentiating Eq. (2) with respect to x and substituting for $\partial T/\partial x$ in Eq. (1) yields:

$$\frac{\partial^2 \theta(x,t)}{\partial x^2} = \frac{\rho}{G} \frac{\partial^2 \theta(x,t)}{\partial t^2} \tag{3}$$

Also differentiating Eq. (2) twice with respect to t results in:

$$\frac{\partial^3 \theta(x,t)}{\partial x \partial t^2} = \frac{1}{GJ} \frac{\partial^2 T(x,t)}{\partial t^2} \tag{4}$$

Moreover, differentiating Eq. (1) with respect to x gives:

$$\frac{\partial^2 T(x,t)}{\partial x^2} = \rho J \frac{\partial^3 \theta(x,t)}{\partial x \partial t^2} \tag{5}$$

and substituting Eq. (4) into (5) results in:

$$\frac{\partial^2 T(x,t)}{\partial x^2} = \frac{\rho}{G} \frac{\partial^2 T(x,t)}{\partial t^2} \tag{6}$$

Eqs. (3) and (6) are the main equations of torsional vibration of the shaft. Assuming zero initial conditions, Laplace transformation of Eqs. (6) and (3) gives:

$$\frac{\partial^2 T(s,t)}{\partial x^2} - \frac{\rho}{G} s^2 T(s,t) = 0$$
$$\frac{\partial^2 \theta(s,t)}{\partial x^2} - \frac{\rho}{G} s^2 \theta(s,t) = 0 \tag{7}$$

where s is the Laplace transform variable. Eq. (7) can be written in the compact form as follows:

$$\frac{\partial^2 k}{\partial x^2} - \Gamma^2 k = 0 \tag{8}$$

In which, k is the main function as:

$$k = \theta(x,s) \text{ or } T(x,s) \tag{9}$$

and

$$\Gamma = s\sqrt{\frac{\rho}{G}} \tag{10}$$

The general solution of Eq. (8) is given by:

$$k = r_1 e^{\Gamma x} + r_2 e^{-\Gamma x} \tag{11}$$

where:

$$e^{\Gamma x} = \cosh \Gamma x + \sinh \Gamma x$$
$$e^{-\Gamma x} = \cosh \Gamma x - \sinh \Gamma x \tag{12}$$

Therefore, the solution for k can be rewritten as:

$$k = (r_1 + r_2)\cosh \Gamma x + (r_1 - r_2)\sinh \Gamma x \tag{13}$$

Hence, the solution of Eqs. (7) will be in the following form:

$$T(x,s) = A\cosh \Gamma x + B\sinh \Gamma x$$
$$\theta(x,s) = C\sinh \Gamma x + D\cosh \Gamma x \tag{14}$$

The unknown constants of integration, A and D, are obtained by imposing the boundary conditions at x=0. That is,

$$A = T(0,s)$$
$$D = \theta(0,s) \tag{15}$$

Next, it remains to find B and C in Eqs. (14). Differentiating Eqs. (14) with respect to x and substituting for $\partial T/\partial x$ and $\partial \theta/\partial x$ from Laplace transformation of Eqs. (1) and (2), respectively, gives:

$$\rho J s^2 \theta(x,s) = A\Gamma \sinh \Gamma x + B\Gamma \cosh \Gamma x$$
$$\frac{1}{GJ} T(x,s) = C\Gamma \cosh \Gamma x + D\Gamma \sinh \Gamma x \tag{16}$$

Upon substitution of x=0 in Eqs. (16), the following results would be obtained:

$$\begin{aligned} B &= sJ\sqrt{\rho G}\ \theta(0,s) = \xi\,\theta(0,s) \\ C &= \frac{1}{sJ\sqrt{\rho G}}T(0,s) = \frac{1}{\xi}T(0,s) \end{aligned} \tag{17}$$

Hence, the solution of Eqs. (7) for the *jth* element can be expressed in the matrix form as follows:

$$\begin{Bmatrix} T_j(x,s) \\ \theta_j(x,s) \end{Bmatrix} = \begin{bmatrix} \cosh\Gamma_j x & \xi_j \sinh\Gamma_j x \\ \dfrac{1}{\xi_j}\sinh\Gamma_j x & \cosh\Gamma_j x \end{bmatrix} \begin{Bmatrix} T_j(0,s) \\ \theta_j(0,s) \end{Bmatrix} \tag{18}$$

where

$$\xi_j = sJ_j\sqrt{\rho_j G_j} \tag{19}$$

According to Fig. 2, for the *jth* element at x=0 there would be:

$$\begin{aligned} T_j(0,s) &= T_{j-1}(s) \\ \theta_j(0,s) &= \theta_{j-1}(s) \end{aligned} \tag{20}$$

Therefore, the main matrix for the distributed element representative of torsional vibration is as follows:

$$\begin{Bmatrix} T_j(s) \\ \theta_j(s) \end{Bmatrix} = \begin{bmatrix} \cosh\Gamma_j l_j & \xi_j \sinh\Gamma_j l_j \\ \dfrac{1}{\xi_j}\sinh\Gamma_j l_j & \cosh\Gamma_j l_j \end{bmatrix} \begin{Bmatrix} T_{j-1}(s) \\ \theta_{j-1}(s) \end{Bmatrix}$$

which can be expressed as:

$$\begin{Bmatrix} T \\ \theta \end{Bmatrix}_j = \left[T_D\right]_j \begin{Bmatrix} T \\ \theta \end{Bmatrix}_{j-1} \tag{21}$$

while:

$$\left[T_D\right]_j = \begin{bmatrix} \cosh\Gamma_j l_j & \xi_j \sinh\Gamma_j l_j \\ \dfrac{1}{\xi_j}\sinh\Gamma_j l_j & \cosh\Gamma_j l_j \end{bmatrix}$$

which is the main transfer matrix for the torsional vibration of distributed element in DLMT.

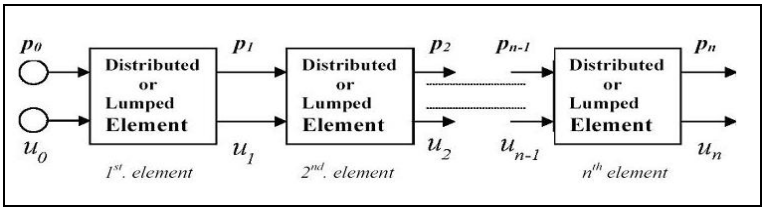

Fig. 1
General series representation of a distributed lumped parameter system (hybrid model).

2.2 The transfer matrix for lumped element

The equation of motion and continuity conditions in Laplace domain of the *jth* lumped element, which is exposed to the applied force *f* in the radius *r* are written as:

$$\begin{aligned} T_j(s) - T_{j-1}(s) + f_j(s) r_j &= J_j^d s^2 \theta_j(s) \\ \theta_j(s) &= \theta_{j-1}(s) \end{aligned} \tag{22}$$

where J_j^d is the mass polar moment of inertia for disk and *r* is the radius which the force is applied. Therefore, Eq. (22) can be expressed in the matrix form as:

$$\begin{Bmatrix} T_j(s) \\ \theta_j(s) \end{Bmatrix} = \begin{bmatrix} 1 & J_j^d s^2 \\ 0 & 1 \end{bmatrix} \begin{Bmatrix} T_{j-1}(s) \\ \theta_{j-1}(s) \end{Bmatrix} + \begin{Bmatrix} -f_j r \\ 0 \end{Bmatrix} \tag{23}$$

In the absence of the force *f*, the matrix form can be expressed as:

$$\begin{Bmatrix} T \\ \theta \end{Bmatrix}_j = \left[T_L\right]_j \begin{Bmatrix} T \\ \theta \end{Bmatrix}_{j-1} \tag{24}$$

while:

$$\left[T_L\right]_j = \begin{bmatrix} 1 & J_j^d s^2 \\ 0 & 1 \end{bmatrix}$$

which is the main transfer matrix for the torsional vibration of lumped element in DLMT.

According to Fig. 1, a shaft with multiple elements can be considered as a vibrating system with various types of distributed and lumped elements, and the overall transfer matrix of the system is obtained by putting these elements together, based on their order and physical properties.

3 ILLUSTRATIVE EXAMPLE AND VERIFICATION

In this section, the methodology outlined previously is applied to a shaft with a disk in its middle (see Fig. 2), which is a simplified model for common industrial systems. The results are then compared with the FEM solution. The properties of the system considered here are shown in Table 1. As mentioned already, the present method can be used for analyzing systems with any number of distributed and lumped elements without any increase in difficulty.

Table 1
Properties of the propeller shaft model.

Parameter	Quantity
Shaft Overall Length $2l$	4 m
Shaft Diameter d	0.150 m
Density of Shaft Material ρ	7800 kg/m^3
Modulus of Elasticity for Shaft E	200 GPa
Shear Modulus of Shaft G	80 GPa
Disk Thickness t	0.080 m
Disk Radius r	1 m
Disk Mass	100 kg
Disk Moment of Inertia	50 kgm^2

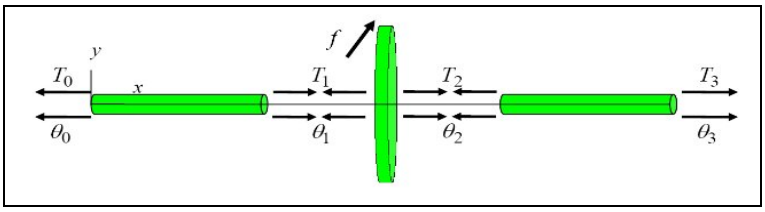

Fig. 2
General model of rotating shaft system.

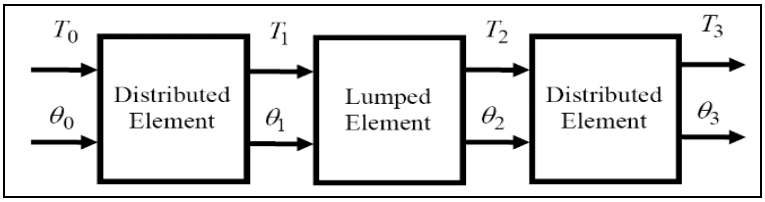

Fig. 3
Hybrid model of rotating shaft system.

3.1 The DLMT solution

To represent the main hybrid model of the system, it should be noticed that the system is combined of two distributed and one lumped elements (Fig. 3). For the distributed elements 1 and 3 the transfer matrices can be written according to Eq. (16) as:

$$\begin{Bmatrix} T_1 \\ \theta_1 \end{Bmatrix} = [T_D]_1 \begin{Bmatrix} T_0 \\ \theta_0 \end{Bmatrix}, \quad \begin{Bmatrix} T_3 \\ \theta_3 \end{Bmatrix} = [T_D]_3 \begin{Bmatrix} T_2 \\ \theta_2 \end{Bmatrix} \tag{25}$$

where:

$$[T_D] = \begin{bmatrix} \cosh \Gamma l & \xi \sinh \Gamma l \\ \dfrac{1}{\xi} \sinh \Gamma l & \cosh \Gamma l \end{bmatrix} \tag{26}$$

In addition, the transfer matrix for the lumped element is:

$$\begin{Bmatrix} T_2 \\ \theta_2 \end{Bmatrix} = [T_L]_2 \begin{Bmatrix} T_1 \\ \theta_1 \end{Bmatrix} \tag{27}$$

where:

$$[T_L]_2 = \begin{bmatrix} 1 & J_2^d s^2 \\ 0 & 1 \end{bmatrix} \tag{28}$$

Substituting Eq. (25) into (27) yields [13,14]:

$$\begin{Bmatrix} T_3 \\ \theta_3 \end{Bmatrix} = \begin{bmatrix} \cosh 2\Gamma l + \dfrac{1}{2} J_2^d \xi^{-1} s^2 \sinh 2\Gamma l & \xi \sinh 2\Gamma l + J_2^d s^2 \cosh^2 \Gamma l \\ \xi^{-1} \sinh 2\Gamma l + J_2^d \xi^{-2} s^2 \sinh^2 \Gamma l & \cosh 2\Gamma l + \dfrac{1}{2} J_2^d \xi^{-1} s^2 \sinh 2\Gamma l \end{bmatrix} \begin{Bmatrix} T_0 \\ \theta_0 \end{Bmatrix} \tag{29}$$

Eq. (23) may be shown in the simple form as follows:

$$\begin{Bmatrix} T_3 \\ \theta_3 \end{Bmatrix} = [T] \begin{Bmatrix} T_0 \\ \theta_0 \end{Bmatrix} \tag{30}$$

where:

$$[T] = \begin{bmatrix} \cosh 2\Gamma l + \frac{1}{2} J_2^d \xi^{-1} s^2 \sinh 2\Gamma l & \xi \sinh 2\Gamma l + J_2^d s^2 \cosh^2 \Gamma l \\ \xi^{-1} \sinh 2\Gamma l + J_2^d \xi^{-2} s^2 \sinh^2 \Gamma l & \cosh 2\Gamma l + \frac{1}{2} J_2^d \xi^{-1} s^2 \sinh 2\Gamma l \end{bmatrix} \tag{31}$$

Eq. (31) is the transfer matrix of the overall system relating torsional moments and torsional angle of the left and right end of the system.

The Laplace transform variable '*s*', in general, is the representative of equation $s=\sigma+i\omega$; in which the real part (σ) shows damping, and the imaginary part ($i\omega$) shows vibrating frequency. It is assumed in the present example that $\sigma=0$ and, therefore; Eq. (24) will be altered from the Laplace domain into the frequency domain by putting $s=i\omega$ [27].

3.2 *Numerical results and discussions*

For each set of boundary conditions, one characteristic equation can be obtained that its solutions will give the natural frequencies of the system.

Assuming that the shaft is clamped at position zero, and free at position 3, the boundary conditions will be (see Fig. 3):

$$\begin{aligned} &T_0 = 0 \quad (at\ clamped\ end) \\ &\theta_3 = 0 \quad (at\ \ free\ end) \end{aligned} \tag{32}$$

According to the above relations, Eq. (24) can be arranged as:

$$\begin{Bmatrix} T_0 \\ \theta_3 \end{Bmatrix} = \begin{bmatrix} \frac{1}{T_{11}} & -\frac{T_{12}}{T_{11}} \\ \frac{T_{21}}{T_{11}} & -\frac{T_{21}T_{12}}{T_{11}} + T_{22} \end{bmatrix} \begin{Bmatrix} T_3 \\ \theta_0 \end{Bmatrix} \tag{33}$$

where u_0 and p_3, are the inputs and u_3 and p_0 are the outputs of the system.

In this case, the natural frequencies are obtained by plotting θ_3/T_3 or θ_3/θ_0, for instance, as shown in Fig. 4. In this view, the natural frequencies occur at the peaks of the spectrum. From Eq. (33), it is clear that the peaks are the result of the denominator approaching zero. Since in all relations, T_{11} is the denominator, the natural frequencies are the roots of T_{11}.

Other than that, putting the relations (32) in Eq. (30) gives:

$$\begin{aligned} &T_{11}T_0 = 0 \\ &T_{21}T_0 = \theta_3 \end{aligned} \tag{34}$$

The first equation is satisfied when $T_{11}=0$, which is another reason for computing the roots of T_{11} to find the natural frequencies as well. The results for this case are listed in Table 2.

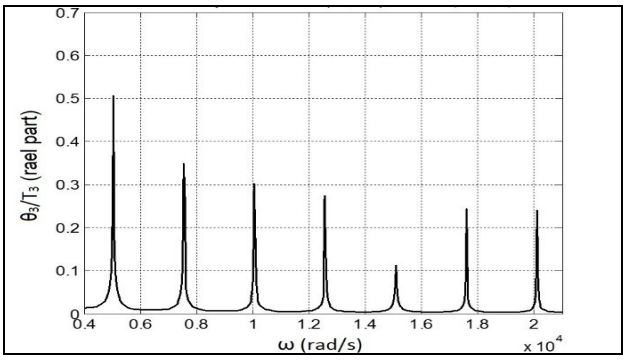

Fig. 4
Frequency spectrum for clamped-free BCs (θ_3/T_3 vs. ω(rad/s)).

Table 2
Natural frequencies of clamped-free rotating system.

Frequency No.	DLMT Method (*Hz*)	FEM Method (*Hz*)	Holzer Method (*Hz*)	% Error (FEM with respect to DLMT)	% Error (Holzer method with respect to DLMT)
1	31.4	31.7	31.4	0.37	1.50
2	397.9	410.0	383.4	3.06	3.64
3	795.8	816.6	798.6	2.60	0.35
4	1193.7	1224.0	1134.8	2.50	4.93
5	1591.5	1632.0	1576.6	2.54	1.00
6	1989.4	2040.0	1862.1	2.54	6.40
7	2403.2	2449.0	2315.7	1.91	3.64
8	2875.2	2859.0	2548.8	2.65	8.48
9	3199.0	3270.0	2996.0	2.22	6.34

3.3 *FEM solution*

To contrast and confirm the results with another method, the finite element method is used to investigate the natural frequencies. The system is modeled by ANSYS software, and meshed using brick 45 (8 nodes 3D) elements (Fig. 5). Block Lanczos solver of ANSYS is used in the analysis. The natural frequencies are listed in Table 2. In addition, the first 4 mode shapes for clamped-free boundary conditions are shown in Figs. 6-9.

According to Table 2, there is less than 2% error between the results of the hybrid modeling method and the results of the FEM solution. The example results verify the results of the new method and approve the accuracy of them as well. They also show the simplicity of modeling the structural and industrial systems with any BCs.

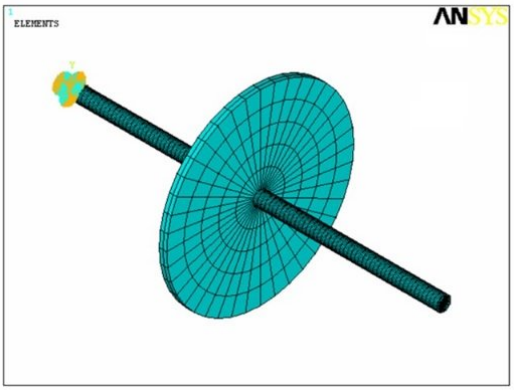

Fig. 5
Meshed clamped-free system.

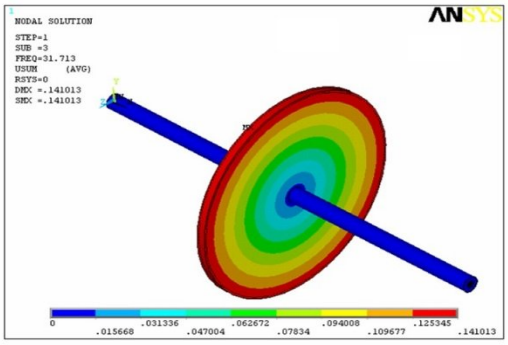

Fig. 6
First mode shape for clamped-free BCs.

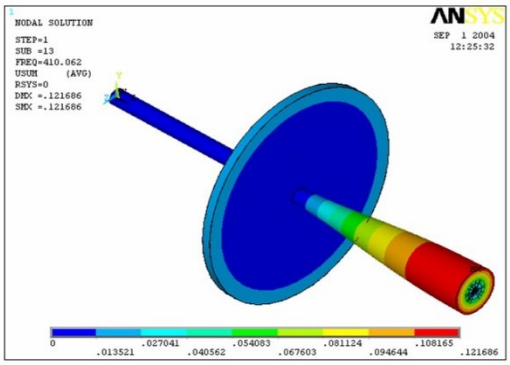

Fig. 7
Second mode shape for clamped-free BCs.

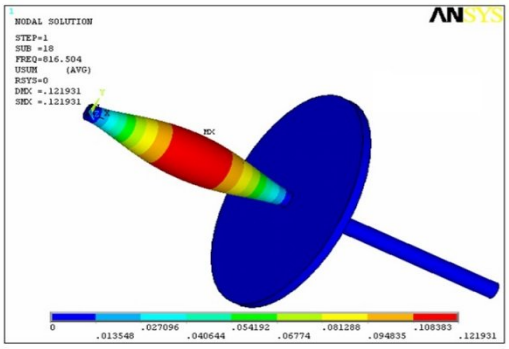

Fig. 8
Third mode shape for clamped-free BCs.

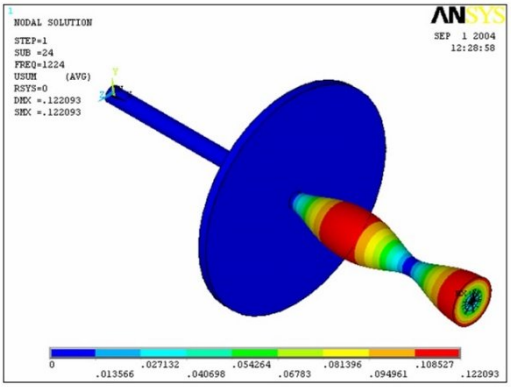

Fig. 9
Fourth mode shape for clamped-free BCs.

4 THE PROPELLER SHAFT ANALYSIS

The vibration study of propeller shaft systems is very significant in the design of shafts for marine crafts, especially ships. The operating speed of these systems should be kept far from their natural frequencies. Furthermore, any redundant vibration or noise makes clear the position of underwater vehicles and leads to unwanted dangers. According to the significance and wide application of propeller shafts in submarines and ships, developing an accurate method of vibration analysis is of great importance. Hence; the exact methods, such as the DLMT, are more appropriate than the approximate ones, such as the TMM.

4.1 *The distributed- lumped modeling analysis*

The propeller shaft system studied in this paper is based on the model presented in Fig. 10. In this figure, "*D*" and "*L*" refer to the distributed and lumped elements, respectively. The geometrical and physical properties of the shaft and disk (propeller model) are presented in Table 3.

Table 3
Properties of the propeller shaft model.

Parameter	Quantity
Shaft Overall Length l	7 m
Shaft Diameter d	0.160 m
Density of Shaft Material ρ	7850 kg/m^3
Modulus of Elasticity for Shaft E	210 GPa
Shear Modulus of Shaft G	80 GPa
Flange Thickness t	0.030 m
Propeller Diameter d	0.750 m
Propeller Mass M_{prop}	1250 kg
Propeller Moment of Inertia J_{prop}	250 kgm^2

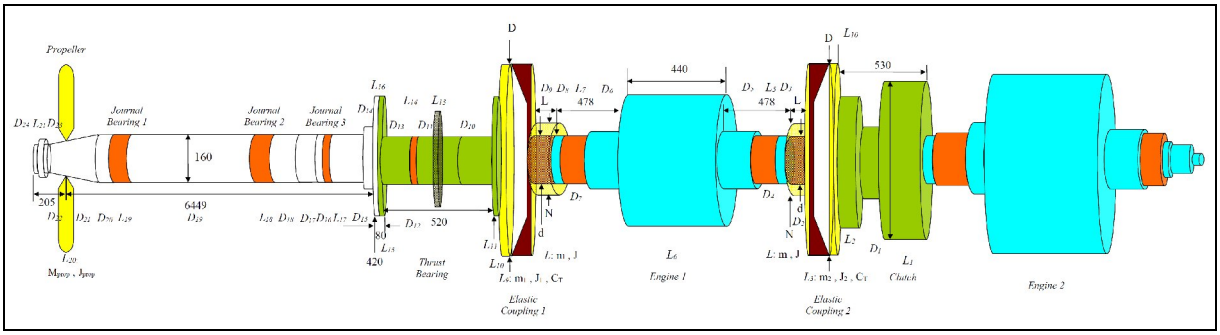

Fig. 10
Model of marine propeller shaft system.

As shown in Fig. 10, the propeller shaft consists of 3 bearings, which has no effect on the torsional vibration. Engine 1 contains a coil shaft with bearings, which are modeled as shafts and disks here. The elastic couplings are modeled as torsional springs with k_t=1.15×10^6 Nm/rad. The clutch after elastic coupling 2 is attached to engine 2, which is the main engine. Engine 2 contains a massive structure, and therefore; the whole shaft system (before the engine) can be assumed as fixed support here.

The flange coupling consists of 2 disks assumed as lumped elements. The propeller is modeled as a disk, in which the thickness and radius are set in such a way that the disk possesses the same mass and moment of inertia as the propeller. The transfer matrix for this system is obtained as follows:

$$[T]=[T]_{Clutch}\times[T]_{Ecoupling2}\times[T]_{Engine1}\times[T]_{Ecoupling1}\times[T]_{Thrust\,Bearing}\times[T]_{Shaft}\times[T]_{Propeller}\times[T]_{Nut} \tag{35}$$

The linear spring, which is representative of oil film; is modeled in the following form:

$$\begin{Bmatrix} T_0 \\ \theta_0 \end{Bmatrix} = \begin{bmatrix} 1 & 0 \\ 1/k_t & 1 \end{bmatrix} \begin{Bmatrix} T_1 \\ \theta_1 \end{Bmatrix} \tag{36}$$

Therefore, the system consisting of spring (the representative of oil film) and mass (the model of thrust disk) can be displayed as follows:

$$\begin{Bmatrix} T_0 \\ \theta_0 \end{Bmatrix} = \begin{bmatrix} 1 & 0 \\ 1/k_t & 1 \end{bmatrix} \begin{bmatrix} 1 & J_d s^2 \\ 0 & 1 \end{bmatrix} \begin{Bmatrix} T_2 \\ \theta_2 \end{Bmatrix} = \begin{bmatrix} 1 & -J_d\omega^2 \\ \dfrac{1}{k_t} & -\dfrac{J_d}{k_t}\omega^2 + 1 \end{bmatrix} \begin{Bmatrix} T_2 \\ \theta_2 \end{Bmatrix} \tag{37}$$

Eq. (30) is the main equation for the torsional vibration of the system which relates left and right ends together. The BCs are considered fixed-free ends which results in the following frequency equation:

$$\begin{Bmatrix} T_0 \\ 0 \end{Bmatrix}_{clamped\ end} = \begin{bmatrix} T_{11} & T_{12} \\ T_{21} & T_{22} \end{bmatrix} \begin{Bmatrix} 0 \\ \theta_n \end{Bmatrix}_{free\ end} \tag{38}$$

Therefore:

$$T_{22}=0 \tag{39}$$

Table 4 shows the torsional natural frequencies of the propeller shaft using the distributed-lumped modeling technique.

4.2 *The FEM analysis*

In order to compare and confirm the results, the finite element method is used to investigate the natural frequencies and mode shapes of the propeller shaft. Here, KissSoft software is employed to obtain the frequencies and mode shapes. The propeller and flanges are modeled as disks. Fig. 11 shows the KissSoft model. The natural frequencies obtained by this method are presented in Table 4. The first 5 mode shapes for the system are shown in Figs. 12-16. According to Table 4, there is a close agreement between the results of the DLMT and FEM in this case.

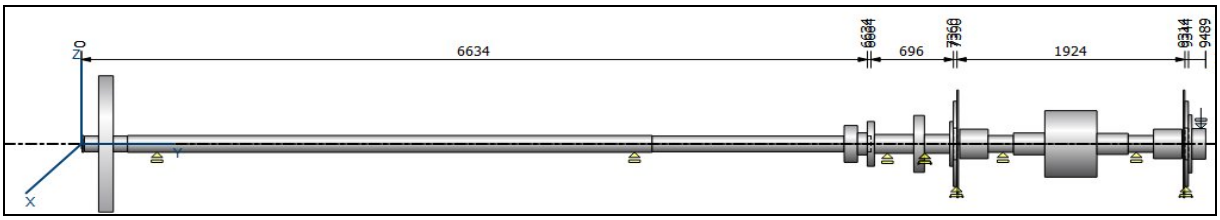

Fig. 11
The model and boundary conditions.

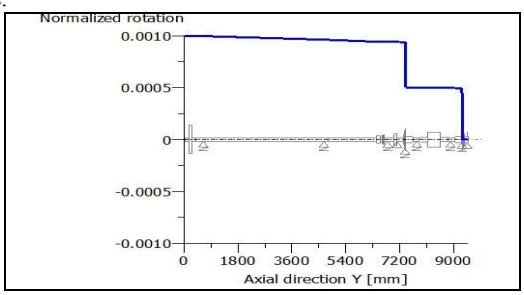

Fig. 12
The first mode shape.

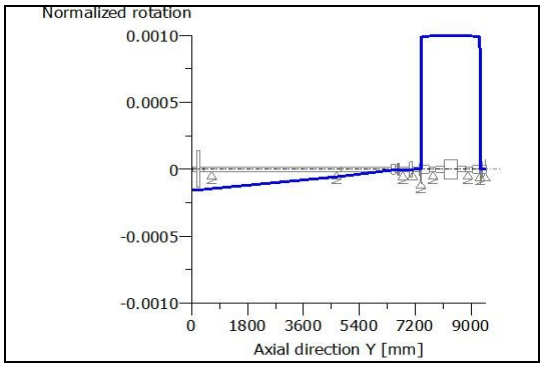

Fig. 13
The second mode shape.

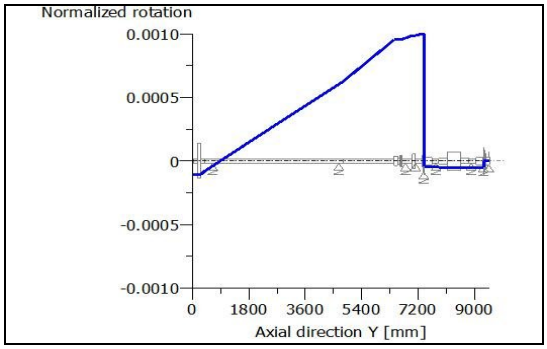

Fig. 14
The third mode shape.

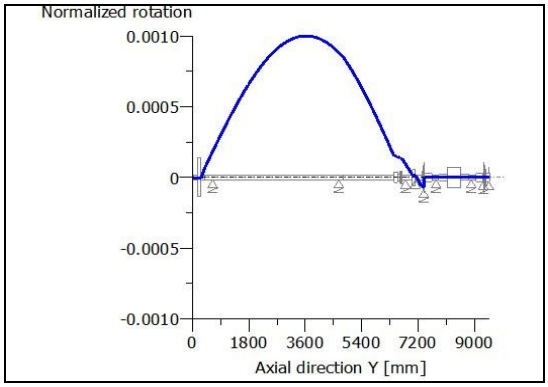

Fig. 15
The fourth mode shape.

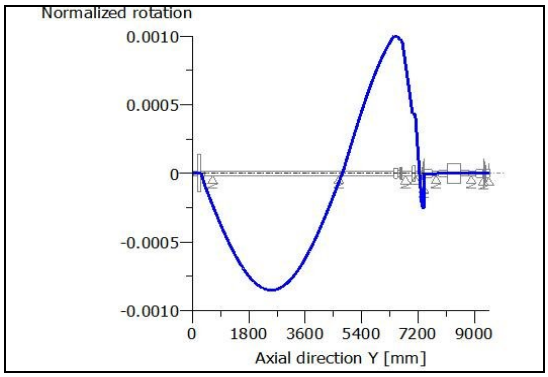

Fig. 16
The fifth mode shape.

Table 4
Natural frequencies of the propeller shaft system (Hz).

Frequency Number	DLMT	FEM	%Error (FEM with respect to DLMT)
1	2.10	2.05	2.4
2	8.60	8.32	2.3
3	27.80	27.42	1.4
4	235.50	233.50	0.9
5	352.50	350.10	0.7

4.3 *The sensitivity analysis*

In this section, the sensitivity analysis for 5 parameters, namely elastic coupling stiffness, propeller moment of inertia, end clutch (base) stiffness, main shaft length and diameter are investigated.

Figs. 17 and 18 show the first 3 natural frequency changes due to the ±50% variations of elastic couplings 1 and 2 stiffness values, respectively. According to these figures, it can be seen that the coupling stiffness value greatly affects the first and second frequency values of the system, while its effect on the third frequency is negligible. Investigating the mode shapes reveals that the first and second mode shapes respectively relate to the oscillation of the propeller and engine with respect to the shaft while the third one relates to the shaft torsional vibration itself. Therefore, the elastic couplings act as springs attached to the vibrating shaft system and has more effects on the first 2 frequencies, while for the third mode shape, the shaft itself vibrates and the spring has less effect; conclusively. It is also clear that the elastic coupling 2 has more effects on the first two frequency values.

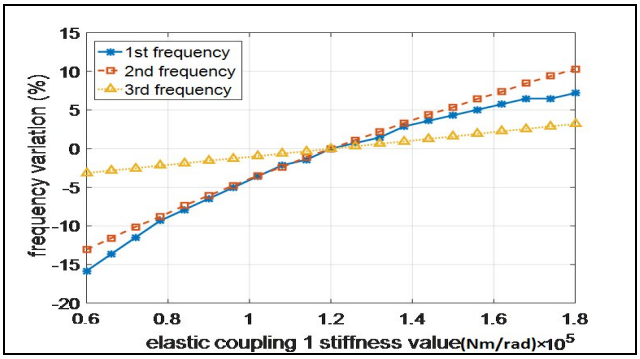

Fig. 17
Frequency variation (%) with respect to the elastic coupling 1 stiffness changes.

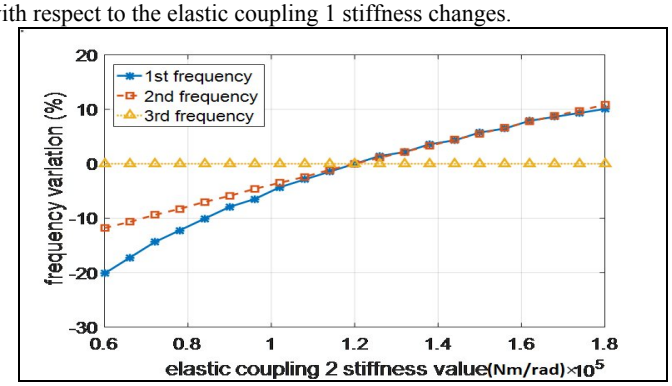

Fig. 18
Frequency variation (%) with respect to the elastic coupling 2 stiffness changes.

Fig. 19 shows the effect of ±50% propeller moment of inertia variations on the first 3 natural frequencies. It is depicted that the propeller inertia moment has the most effect on the first frequency value of the system (about +30% - -20% variations), and its effect on the higher frequencies is reduced. This is because the first mode shape relates to the oscillation of the propeller with respect to the shaft. The figure also shows that increasing the propeller mass brings more frequency changes compared with the decreasing of its value.

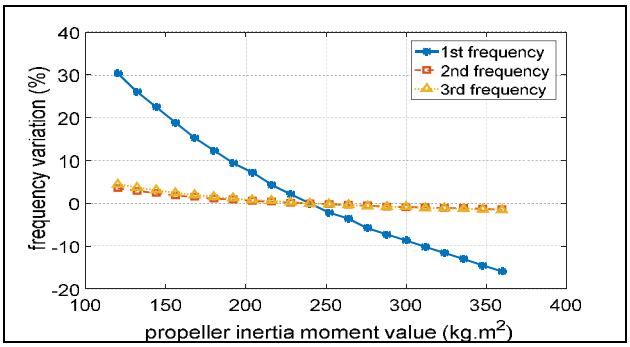

Fig. 19
Frequency variation (%) with respect to the propeller moment of inertia changes.

The effect of the main (propeller) shaft length on the first 3 frequencies is displayed in Fig. 20. According to this figure, ±50% variations of shaft length value change the third frequency between +30% and -15%. While its effect on the first 2 frequencies is negligible. The reason is that the third mode shape relates to the oscillation of the shaft itself, while the first and second ones relate to the vibration of the propeller and engine, respectively. It also shows that decreasing the shaft length has more effect on the frequency values in contrast with the increasing of its value.

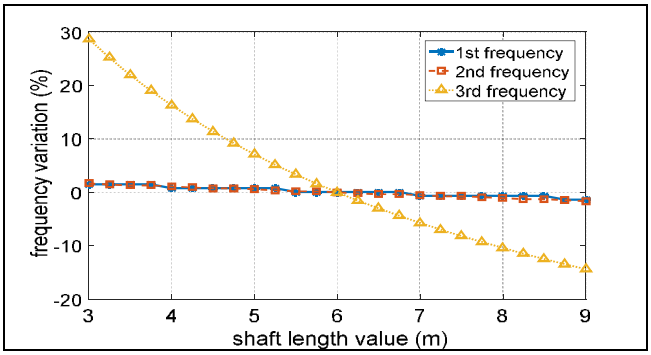

Fig. 20
Frequency variation (%) with respect to the shaft length changes.

Fig. 21 shows the first 3 natural frequency changes due to the ±50% variations of main (propeller) shaft diameter. According to this figure, it can be seen that the shaft diameter value greatly affects the third frequency value of the system (about -60% - +80% variations), while it has less effect on the first 2 frequency values (about -25% - +5%). The main reason is that the third mode shape relates to the oscillation of the shaft itself. It also can be seen that increasing the shaft diameter would increase the frequency values, and vice versa.

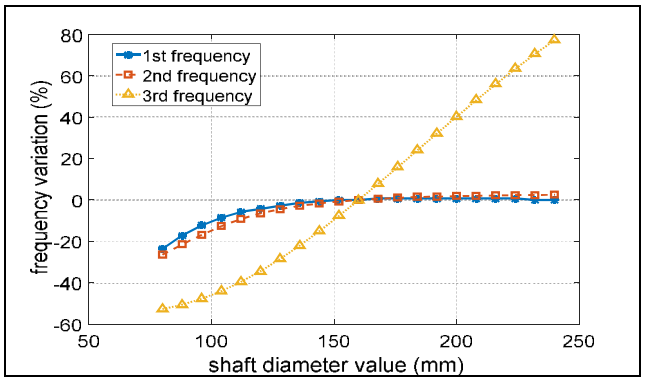

Fig. 21
Frequency variation (%) with respect to the shaft diameter changes.

The effects of structural stiffness (engine 2 stiffness) value on the first 3 natural frequencies are investigated in Fig. 22. Since the clutch is attached to the main engine with enormous mass and moment of inertia, the final support of the system is not exactly the fixed one and could be modeled by a spring [15, 29].

This figure shows that changing the base stiffness value from 10^7 to 10^8 brings less than 1% variations for the first 2 frequencies, and about 7% variations for the third frequency with respect to the fixed support. In addition, it can be seen that the base stiffness has a negligible effect on the higher frequencies. Therefore, assuming fixed support brings little errors and thus gives acceptable results.

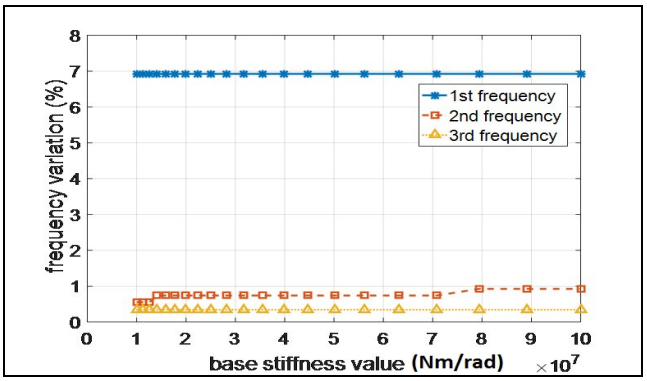

Fig. 22
Frequency variation (%) with respect to the base stiffness variations.

5 CONCLUSIONS

In this paper, the shaft torsional equation of motion is solved by the analytical method. Considering the distributed lumped modeling technique (DLMT), the transfer matrix for the distributed element is presented by applying the proposed method. The transfer matrix for the lumped elements is also obtained using hybrid modeling.

The natural frequencies obtained by DLMT are compared and verified with the results of FEM for the rotor shaft with a disk in the middle. The technique is also applied to calculate the frequencies of a marine propeller shaft system modeled as a shaft with different supports carrying the propeller and flanges as lumped elements. The frequencies obtained by DLMT are compared with the results of the finite element method, using KissSoft software. The mode shapes of the propeller shaft model are also obtained by KissSoft software. As shown in Table 4, the two methods differed by less than 1 percent which confirms the DLMT results.

The sensitivity analysis for elastic coupling stiffness, propeller moment of inertia, end clutch (base) stiffness, main shaft length and diameter are also investigated. It is shown that the elastic coupling 2 and the propeller moment of inertia have the most effects on the first natural frequency, and the shaft length and diameter have the most effects on the higher frequencies.

The results presented herein show that the natural frequencies and mode shapes of the torsional vibration of a complicated shaft with various supports and flanges can be computed effectively using the distributed-lumped modeling technique. Moreover, since the method is closely related to the governing partial differential equations for the system, accurate results are achieved. In this way, the simplicity and accuracy of this method bring proper application for complicated systems.

REFERENCES

[1] R.B. Randall, Vibration- Based Condition Monitoring: Industrial, Aerospace and Automotive Applications, John Wiley & Sons Inc (2011).
[2] S. Talebi, H. Uosofvand, A. Ariaei, Vibration analysis of a rotating closed section composite timoshenko beam by using differential transform method, Applied and Computational Mechanics, 1(4), 181-186 (2015).
[3] A. Halilbese, O.A. Ozsoysal, The coupling effect on torsional and longitudinal vibrations of marine propulsion shaft system, Journal of ETA Maritime Science, 9(4), 274-282 (2021).

[4] Q. Huang, X. Yan, C. Zhang, H. Zhu, Coupled transverse and torsional vibrations of the marine propeller shaft with multiple impact factors, Ocean Engineering, 178, 48–58 (2019).
[5] D. Li, Y. Du, Y. Tian, Analysis of vibration characteristics of ship propeller spindle, Vibroengineering Procedia, 56, 1-7(2024).
[6] A. Madokuboye, A.E. Ogbonnaya, Vibration analysis of a 3-bladed marine propeller shaft for 35000DWT bulk carrier, European Journal of Engineering Research and Science, 4(10), 78-86 (2019).
[7] M. Sadab, S. Kundu, Dispersive behavior of SH waves in a smart composite structure of viscoelastic media, Wave Motion, 130, 103355 (2024).
[8] M. Sadab, S. Kundu, Analysis of love-type wave in a piezoelectric layer bonded between fiber-reinforced viscoelastic and dual porous media, Waves in Random and Complex Media, 1–20 (2024).
[9] M. Sadab, S. Kundu, Love wave propagation in a piezoelectric layer imperfectly bonded over a cracked porous half-space, Journal of Vibration and Control, 30(11-12), 2775-2785 (2023).
[10] R. Whalley, The response of distributed-lumped parameter systems, Proceedings of IMechE, 202(C6), 421-428 (1988).
[11] M. Aleyaasin, M. Ebrahimi R. Whalley, Flexural vibration of rotating shafts by frequency domain hybrid modeling, Computers and Structures, 79, 319-331(2001).
[12] S. Soheili M. Abachizadeh, Flexural vibration of multistep rotating timoshenko shafts using hybrid modeling and optimization techniques, Vibration and Control, 29(7-8), 1833–1849 (2022).
[13] M. Tahani, S. Soheili, M. Abachizadeh, A. Farshidianfar, Rotors frequency and time response of torsional vibration using hybrid modeling, 16th Annual Conference of Mechanical Engineering (ISME), Kerman, Iran (2008).
[14] M. Tahani, S. Soheili, Frequency and time response of rotors longitudinal vibration using hybrid modeling, 13th Annual (International) Conference of Mechanical Engineering (ISME), Isfahan, Iran (2005).
[15] L. Murawski, A. Charchalis, Simplified method of torsional vibration calculation of marine power transmission system, Marine Structures, 39, 335–349 (2014).
[16] H.S. Han, K.H. Lee, S.H. Park, Estimate of the fatigue life of the propulsion shaft from torsional vibration measurement and the linear damage summation law in ships, Ocean Engineering, 107, 212–221(2015).
[17] L. Brydum, S.B. Jakobsen, Vibration characteristics of two-stroke, low speed diesel engines, International Marine Propulsion Conference, 9th, MAN B&W Diesel a/s, Copenhagen, 1-16, London (1987).
[18] Y. Huang, C. Horng, Analysis of torsional vibration systems by the extended transfer matrix method, Journal of Vibration and Acoustics, 121, 250-255 (1999).
[19] J.S. Wu, I.H. Yang, Computer method for torsion-and-flexure coupled forced vibration of shafting system with damping, Journal of Sound and Vibration, 180, 417-435 (1995).
[20] Q. Huang, X. Yan, Y. Wang, Numerical and experimental analysis of coupled transverse and longitudinal vibration of a marine propulsion shaft, Journal of Mechanical Science and Technology, 30, 5405-5412 (2016).
[21] L. Murawski, Axial vibrations of a propulsion system taking into account the couplings and boundary conditions, Journal of Marine Science and Technology, 9, 171-181(2004).
[22] I. Senjanovića, I. Ančića, G. Magazinovićb, N. Alujevića, N. Vladimira, D. Choc, Validation of analytical methods for the estimation of the torsional vibrations of ship power transmission systems, Ocean Engineering, 184, 107-120 (2019).
[23] L. Xiang, S. Yang C. Gan, Torsional vibration of a shafting system under electrical disturbances, Shock and Vibration, 19, 1223–1233 (2012).
[24] D. Zou, J. Xu, J. Zhang, F. Lv, N. Ta, Z. Rao, The hydroelastic analysis of marine propellers considering the effect of the shaft, Theory and Experiment, Ocean Engineering, 221, 108547 (2021).
[25] H.S. Han, K.H. Lee, S.H. Park, Parametric study to identify the cause of high torsional vibration of the propulsion shaft in the ship, Engineering Failure Analysis, 59, 334–346 (2016).
[26] J. Firouzi, H. Ghassemi, K. Akbari Vakilabadi, Vibration equations of the coupled torsional, longitudinal, and lateral vibrations of the propeller shaft at the ship stern, Scientific Journals of the Maritime University of Szczecin, 61(133), 121–129 (2020).
[27] S.S. Rao, Mechanical Vibration, Pearson Publications, 6th Edition (2016).
[28] L. Meirovitch, Fundamentals of Vibration, McGraw-Hill Inc (2001).
[29] T.P. Holopainen, P. Jorg, J. Nïiranen, D. Andrea, Electric motors and drives in torsional vibration analysis and design, Proceedings of the Forty-Second Turbomachinery Symposium, Houston, Texas (2013).